Ab-initio calculation of the pressure dependence of phonons and elastic constants for Al and Li

G.J. Vázquez, L.F. Magaña

J. Phys. France **49** (1988) 497-504 MARS **1988**, PAGE 497

Classification
Physics Abstracts
63.20

Ab-initio calculation of the pressure dependence of phonons and elastic constants for Al and Li

G. J. Vázquez and L. F. Magaña

Instituto de Física, Universidad Nacional Autónoma de México, Apdo. Postal 20-364, México, D.F., 01000, Mexico

(*Reçu le 10 juin 1987, accepté le 30 novembre 1987*)

Résumé. — Nous avons calculé les potentiels interioniques pour l'aluminium et le lithium d'après les pseudopotentiels. Nous avons construit ces pseudopotentiels à partir des densités électroniques induites autour des noyaux d'aluminium et de lithium. Ensuite, nous avons calculé les courbes de dispersion de phonons et les constantes élastiques. Nous avons répété ce calcul pour plusieurs valeurs de la pression en changeant à chaque fois la valeur r_s du paramètre de la densité du gaz d'électrons. Les densités électroniques induites ont été calculées en utilisant la théorie de la fonction densité.

Abstract. — We calculated the interionic potentials for aluminium and lithium from first principle pseudopotentials. We constructed these pseudopotentials from the induced electron densities around an aluminium nucleus and around a lithium nucleus respectively. Then we calculated the phonon dispersion curves and the elastic constants. We repeated the whole calculation for several values of pressure by changing, each time, the value of the electron gas density parameter r_s. The induced electron densities were calculated using Density Functional Theory.

1. Introduction.

A good starting point to make predictions of the behaviour of materials under pressure is to have a reliable, pressure dependent interionic potential or a reliable, pressure dependent pseudopotential.

In previous work [1, 2], we had performed a first-principle calculation of the interionic potentials of lithium and aluminium without using pseudopotentials, following a method based on density functional formalism [3, 4], with no adjustable parameters. This method had been applied with success to metallic hydrogen [5, 6]. The phonons generated from those interionic potentials were not satisfactory and were not used to calculate any property of aluminium or lithium under pressure.

In this work we calculated the interionic potential using local, pressure dependent, first-principle pseudopotentials for lithium and aluminium following the method of Manninen *et al.* [7], who followed the work of Rasolt *et al.* [8], with some differences.

With their method Manninen *et al.* [7] could calculate the total energy of the metal, the equilibrium lattice constant, bulk modulus, vacancy formation energy and the electrical resistivity of the liquid phase. They considered aluminium. More recently, Jena *et al.* [9] calculated the phonon dispersion curve of aluminium using the interionic potential reported by Manninen *et al.* [7], obtaining a good agreement with experimental results. In this method, a Fourier transform of the displaced electron density, around an impurity in an electron gas, is taken. A local pseudopotential is then defined in order to reproduce exactly, in linear response theory, the displaced electronic density around the impurity in the electron gas. In this way, some of the non linear screening effects are included into the pair potential calculated from this pseudopotential [7, 8]. They considered two models [7] to calculate this displaced electronic density. In the first model they calculated the screening of the ion in a homogeneous electron gas. In the second model they considered the ion embedded in a jellium vacancy [7, 10, 11]. It turned out that the second model is much better to describe the cohesion in the metal than the first model. In this work we used the second model to construct the pseudopotential.

We started our present work calculating the screening electron densities for lithium and aluminium by the density functional formalism using the

model of the ion embedded in a jellium vacancy. By smoothing these densities near the ion we obtained the pseudodensities and the pseudopotential. From this pseudopotential we calculated the interionic potential, the phonons and elastic constants as functions of pressure.

From pseudopotential theory and linear response theory [7, 12], the interionic potential is given by :

$$\Phi(r) = \frac{z^2}{r}\left\{1 + \frac{2}{\pi z^2} \times \right. \\ \left. \times \int_0^\infty \frac{dq \sin(qr)\, \varepsilon(q)[\delta n(q)]^2}{q[1-\varepsilon(q)]}\right\}, \quad (1)$$

where z is the charge of the metal ion, $\varepsilon(q)$ is the dielectric function of the electron gas and $\delta n(q)$ is the induced charge pseudodensity. The relationship between the charge pseudodensity and the unscreened pseudopotential form factor, $V(q)$ (which is assumed to be weak) is

$$V(q) = \frac{4\pi\, \delta n(q)\, \varepsilon(q)}{q^2[1-\varepsilon(q)]}. \quad (2)$$

In section 2 we present the equations of the density functional formalism we have solved for the model of the nucleus embedded into a jellium vacancy [7, 10, 11].

Section 3 is used to describe briefly the method of Manninen *et al.* [7] to construct the pseudopotentials from the electron densities and to show the dielectric function we used.

In section 4 we show how we calculated the phonons and the elastic constants.

Section 5 is for results and discussion.

2. Electronic densities.

To calculate the displaced electron densities we use the formalism of Hohenberg-Kohn and Sham [3, 4]. The central result of this formalism states that there exists a one-body local potential, $V_{\text{eff}}(\underline{r})$, which through the one-body Schrödinger equation given by

$$\left[-\frac{1}{2}\nabla^2 + V_{\text{eff}}(\underline{r})\right]\psi_i(\underline{r}) = \varepsilon_i\, \psi_i(\underline{r}), \quad (3)$$

generates the set of wave functions $\psi_i(\underline{r})$ and the exact ground state density of the system through the independent particle density expression :

$$n(\underline{r}) = \sum_{\varepsilon_i < \varepsilon_f} |\psi_i(\underline{r})|^2, \quad (4)$$

where the sum extends up to the Fermi energy.

The effective potential is

$$V_{\text{eff}}(\underline{r}) = -\Phi(\underline{r}) + \frac{\delta E_{\text{xc}}[n(\underline{r})]}{\delta n(\underline{r})}, \quad (5)$$

where $\Phi(\underline{r})$ is the total electrostatic potential of the system, and $E_{\text{xc}}[n(\underline{r})]$ is the exchange-correlation energy of the system.

When we omit gradient corrections it is possible to write

$$\frac{\delta E_{\text{xc}}[n(\underline{r})]}{\delta n(\underline{r})} = \frac{d}{dn}\left[n(\underline{r})\, \varepsilon_{\text{xc}}(n(\underline{r}))\right], \quad (6)$$

where $\varepsilon_{\text{xc}}(n(\underline{r}))$ is the exchange correlation energy per particle in a homogeneous electron gas of density $n(\underline{r})$.

For the exchange-correlation contribution to the effective potential, equation (6), we use the expression given by Gunnarson and Lundquist [13] in atomic units (double Rydbergs) :

$$V_{\text{xc}}(\underline{r}) \frac{\delta E_{\text{xc}}[n(\underline{r})]}{\delta n(\underline{r})} = -0.6109 \times \\ \times \left[\frac{1}{r_s} + 0.0585 \ln\left(1 + \frac{11.4}{r_s}\right)\right] \quad (7)$$

where

$$\frac{4}{3}\pi r_s^3(r) = \frac{1}{n(r)}.$$

In order to have $V_{\text{eff}}(\underline{r})$ vanishing at large r, the exchange-correlation part is rescaled to :

$$V_{\text{xc}}(\underline{r}) \to V_{\text{xc}}[n(\underline{r})] - V_{\text{xc}}[n_0]. \quad (8)$$

The electrostatic potential obeys Poisson's equation

$$\nabla^2\Phi = -4\pi D(\underline{r}), \quad (9)$$

where $D(\underline{r})$ is the total charge density.

If we consider the nucleus as located at the centre of a vacancy in jellium

$$D(\underline{r}) = z\,\delta(\underline{r}) + n_0\,\theta(r - R_{\text{ws}}) - n(\underline{r}), \quad (10)$$

where $\theta(x)$ is the step function, R_{ws} is the Wigner-Seitz radius, z is the ion charge and $\delta(r)$ is the Dirac Delta function.

3. The pseudopotential.

Once we know the Fourier transform of the induced charge pseudodensity, $\delta n(q)$, we can find the unscreened pseudopotential form factor using equation (2). It should be remarked that, in the pseudopotential formulation, the pseudodensity must not have core orbitals. In this way the pseudodensity must not contain wiggles near the ion. The wiggles near the ion would appear because of the orthogonalization of conduction states to core orbitals.

For the case of the nucleus embedded in a jellium vacancy, the induced density is calculated by taking the difference [7]

$$\delta n(\underline{r}) = n(\underline{r}) - n_v(\underline{r}) - 2\sum_b |\psi_b(\underline{r})|^2, \quad (11)$$

where $n(\underline{r})$ is calculated with the total charge

density given by equation (10) and $n_v(\underline{r})$ is the electron density around a jellium vacancy and corresponds to an external positive background charge density

$$D^+(\underline{r}) = n_0\,\theta(r - R_{ws})\,.$$

Charge neutrality requires that :

$$\int \delta n(\underline{r})\,\mathrm{d}v = z\,,$$

where z is the valence of the ion in the metal.

The induced density, calculated from the density functional formalism, contains wiggles at small $\underline{r}$ due to the orthogonalization of conduction states to core orbitals. We have smoothed our calculated induced density, following the method of Manninen *et al.* [7]. This is achieved by using a second-order polynomial given by

$$\delta n(\underline{r}) = A - Br^2 \quad r \leqslant R_0\,, \tag{12}$$

for small values of r. The constants A, B and R_0 are calculated by the conditions that $\delta n(\underline{r})$ and $(\delta/\delta r)[\delta n(\underline{r})]$ are continuous at $r = R_0$ and that the electronic charge is conserved. The smoothed density is the one we used as pseudodensity, $\delta n(q)$, in equation (1) to calculate the interionic potential.

The dielectric function we used satisfies, by construction, the compressibility theorem which is important in connection of the interionic potential [7, 14], and it is given by

$$\varepsilon(q) = 1 + \left(\frac{4\pi}{q^2}\right) G(q)\,, \tag{13}$$

with

$$G(q) = \frac{G_0(q)}{1 - (4\pi/k_{TF}^2)\,G_0(q)(1 - L)}\,, \tag{14}$$

where $G_0(q)$ is the usual Lindhard polarizability, k_{TF} is the Fermi-Thomas screening constant and

$$L = \left(\frac{\partial\mu}{\partial r_s}\right)\Big/\left(\frac{\partial\varepsilon_F}{\partial r_s}\right)\,. \tag{15}$$

In equation (15) is the chemical potential, ε_F is the Fermi energy and

$$\mu(r_s) = \varepsilon_F(r_s) + \mu_{xc}(r_s)\,,$$

where $\mu_{xc}(r_s)$ is the exchange-correlation contribution to the chemical potential.

Using the expression of Gunnarson and Lundquist [13] for exchange-correlation (which we used in the calculation of the induced density), the corresponding value of L is :

$$L = 1 - \left(\frac{1}{9\pi^4}\right)^{1/3} r_s\left[1 + \frac{0.6213\,r_s}{r_s + 11.4}\right]\,. \tag{16}$$

4. Phonons and elastic constants.

Having the induced charge pseudodensity and the dielectric function, we used equation (1) to calculate the interionic potential.

For the interionic potential we calculated the phonon dispersion curves using the harmonic approximation [15, 16] and the self-consistent harmonic approximation [17-19]. In the latter approximation, in contrast with that of Born and Von Kárman [15, 16], there is no initial hypothesis of smallness for the amplitude of atomic vibrations and hence no truncated Taylor series expansion of the interatomic potential energy.

The resulting set of self-consistent equations to solve in order to obtain the phonon dispersion curve in the self-consistent harmonic approximation is the following

$$\omega_\lambda^2(\underline{k})\,\varepsilon_\lambda^\alpha(\underline{k}) = \sum_\beta D_{\alpha\beta}(\underline{k})\,\varepsilon_\lambda^\beta(\underline{k})\,, \tag{17}$$

where $\varepsilon_\lambda^\alpha(\underline{k})$ is the component of the polarization vector $\varepsilon_\lambda(\underline{k})$ and the dynamical matrix is

$$D_{\alpha\beta}(\underline{k}) = \frac{1}{M}\sum_\ell (1 - \cos\,(\underline{k}\,.\,\underline{R}_\ell))\langle\Phi_{\alpha\beta}(\underline{R}_\ell)\rangle\,, \tag{18}$$

with

$$\langle\Phi_{\alpha\beta}(\underline{R}_\ell)\rangle = \frac{1}{(8\pi^3 \det\lambda_\ell)^{\frac{1}{2}}}\int \mathrm{d}^3\mu\,\exp\times$$

$$\times\left(-\frac{1}{2}\sum_{\gamma\delta}\mu_\gamma(\lambda_\ell^{-1})_{\gamma\delta}\,\mu_\delta\right)\Phi_{\alpha\beta}(\underline{R}_\ell + \mu_\ell)\,, \tag{19}$$

where M is the ion mass, $\boldsymbol{\mu}_\ell$ is the vector describing the displacement of atom ℓ from its equilibrium position, $\underline{R}_\ell$, and $\Phi_{\alpha\beta}(\underline{R}_\ell + \boldsymbol{\mu}_\ell)$ is the tensor derivative of the interatomic potential evaluated at $\underline{R}_\ell + \underline{\mu}_\ell$.

Finally :

$$(\lambda_\ell)_{\alpha\beta} = \frac{1}{MN}\sum_{\underline{k}\lambda}(1 - \cos\,(\underline{k}\,.\,\underline{R}_\ell))\,\varepsilon_\lambda^{*\alpha}(\underline{k})\times$$

$$\times\,\varepsilon_\lambda^\beta(\underline{k})\cot h\left(\frac{1}{2}\beta\hbar\omega_\lambda(\underline{k})\right)/\omega_\lambda(\underline{k})\,, \tag{20}$$

where N is the number of ions. The sum is over the first Brillouin zone, β is $1/(k_B T)$, k_B being the Boltzmann constant.

To solve the set of self-consistent equations (17), (18), (19) and (20) we start with the frequencies generated by the Harmonic Approximation as the first trial. Then the convergence procedure is followed.

For lithium (and in general for the alkali metals) the harmonic approximation gives a better description of the phonons than the self-consistent harmonic approximation [20]. This is because the self-consistent harmonic approximation generates frequency

shifts, relative to the harmonic approximation, of the wrong sign [20]. These shifts are practically cancelled when cubic terms are included in the self-consistent harmonic approximation. For aluminium the self-consistent harmonic approximation gives a better description of the phonons than the harmonic approximation.

Following the tensor force model and notation of reference [21], the force matrix, $\Phi_{ij}(S)$, is defined to be the force on the origin atom in the i direction when the atom S moves one unit distance in the j direction. This force matrix is symmetric and its elements are denoted by

$$\Phi_{ij}^{(S)} = \begin{bmatrix} \alpha_1^S & \beta_3^S & \beta_2^S \\ \beta_3^S & \alpha_2^S & \beta_1^S \\ \beta_2^S & \beta_1^S & \alpha_3^S \end{bmatrix} . \tag{21}$$

The point S is one of a set of points according to the symmetry of the lattice. This set of points is denoted by $S = 1, 2, 3$, etc., corresponding to the first shell of neighbours (nearest neighbours), second shell of neighbours, third shell of neighbours, etc. The force matrices of the other members of the set consist of rearrangements of the same set of force constants.

The elastic constants, C_{11}, C_{44}, C_{12} are given by [21]

$$\begin{aligned} aC_{11} &= 8\,\tau \sum_S \frac{n^S}{48} \sum_j (h_j^S)^2\, \alpha_j^S \\ aC_{44} &= 4\,\tau \sum_S \frac{n^S}{48} \sum_j [(h_{j+1}^S)^2 + (h_{j+2}^S)^2]\, \alpha_j^S \\ a(C_{12} + C_{44}) &= 16\,\tau \sum_S \frac{n^S}{48} \sum_j h_{j+1}^S \cdot h_{j+2}^S\, \beta_j^S \end{aligned} \tag{22}$$

where a is the lattice constant, n^S is the number of lattice points for neighbour shell S ; h_j^S corresponds to three non-negative integers such that $h_1 > h_2 > h_3$ and that the coordinates of a point in shell S are $h_1\, a/2$, $h_2\, a/2$, $h_3\, a/2$. For FCC (aluminium), $\tau = 1$ and for BCC (lithium), $\tau = 1/2$.

The relations between the force constants of the tensor force model and the axially symmetric model are [22] :

$$\begin{aligned} \alpha_1^S &= C_B(S) + (h_1^2/h^2)\, k_1(S) \\ \alpha_2^S &= C_B(S) + (h_2^2/h^2)\, k_1(S) \\ \alpha_3^S &= C_B(S) + (h_3^2/h^2)\, k_1(S) \\ \beta_1^S &= (h_2 h_3/h^2)\, k_1(S) \\ \beta_2^S &= (h_3 h_1/h^2)\, k_1(S) \\ \beta_3^S &= (h_1 h_2/h^2)\, k_1(S) \end{aligned} \tag{23}$$

where $h^2 = h_1^2 + h_2^2 + h_3^2$, and $k_1(S)$ and $C_B(S)$ are the two force constants of the axially symmetric model for the S-th shell of neighbours [22].

We could relate easily the force constants $k_1(S)$ and $C_B(S)$ to the derivatives of the interionic potential and we got :

$$k_1(S) = \left[\frac{d^2V(r)}{dr^2} - \frac{1}{r}\frac{dV(r)}{dr} \right]_{(S)} \tag{24}$$

and

$$C_B(S) = \left[\frac{1}{r}\frac{dV(r)}{dr} \right]_{(S)} . \tag{25}$$

In this way, once we knew the interionic potential $V(r)$, we could find $k_1(S)$ and $C_B(S)$ and using equations (22) and (23) we calculated the elastic constants.

For every value of the pressure, i.e., for every value of the electron gas density parameter r_s we have calculated the pseudopotential, the interionic potential, the phonon dispersion curves, the force constants and the elastic constants for lithium and aluminium.

5. Results and discussion.

In figures 1 and 2 we show some of the displaced electron densities and pseudodensities resulting from our calculation.

We calculated the displaced electron densities fully self-consistently. The Schrödinger equation was solved in steps of 0.01 a_0, where a_0 is the Bohr radius ($a_0 = 0.529$ Å), up to $R_{max} = 15.04\, a_0$, where the phase shifts were evaluated for both cases, lithium and aluminium.

The following step was to calculate the Fourier transform of the smoothed densities. Since this implies knowing $\delta n(r)$ up to infinity, we used the

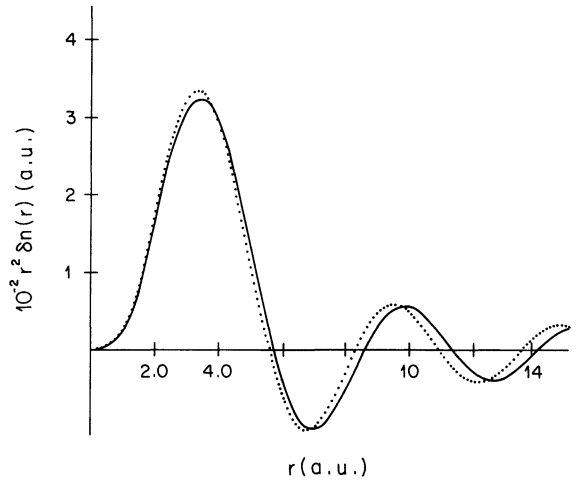

Fig. 1. — Smoothed displaced electron densities for a lithium ion embedded into a jellium vacancy. At atmospheric presure : —— ; for a value of r_s which is 4 % smaller than the corresponding value at atmospheric pressure : . . .

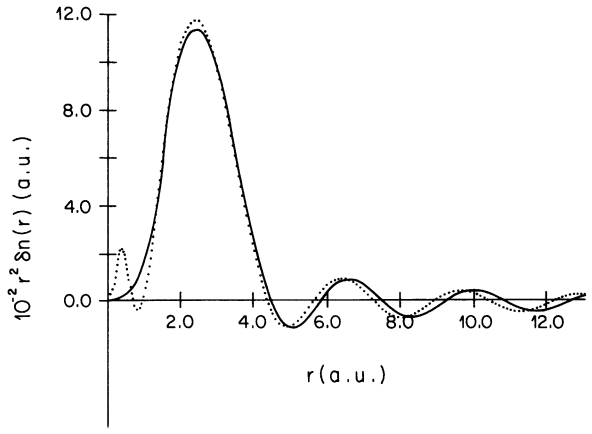

Fig. 2. — Displaced electron densities for an aluminium ion embedded into a jellium vancancy. Smoothed density at atmospheric pressure : —— ; non-smoothed density for a value of r_s which is 4 % smaller than the corresponding value at atmospheric pressure : . . .

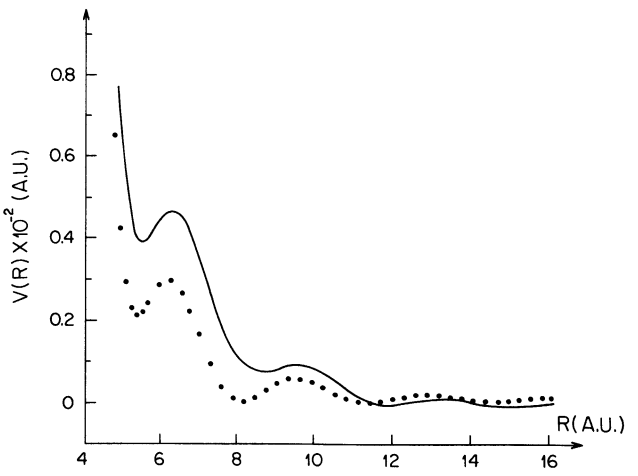

Fig. 4. — Calculated interionic potential for aluminium. For a value of r_s corresponding to atmospheric pressure : —— ; for a value of r_s which is 4 % smaller than the corresponding value at atmospheric pressure : . . .

asymptotic form for $n(r)$ for distances larger than R_{max}, given by

$$\delta n(r) = A \cos (2 k_F r + \phi)/r^3 \qquad (26)$$

where the constants A and ϕ were obtained using the last points in our calculation of $n(r)$. The accuracy of our Fourier transform was tested by taking the inverse Fourier transform of $\delta n(q)$ and the resulting difference with respect to the original values of $\delta n(r)$ was less than 0.1 % in all the cases.

Using $\delta n(q)$ and the dielectric function given by equations (13), (14), (15) and (16), we obtained the interionic potentials by equation (1). Figures 3 and 4 show the resulting interionic potentials for lithium and aluminium respectively for two different values of r_s. We can see that the effect of pressure is to make the shape of the potentials at the position of the first minimum sharper. The frequency of the oscillations of the potentials also increases.

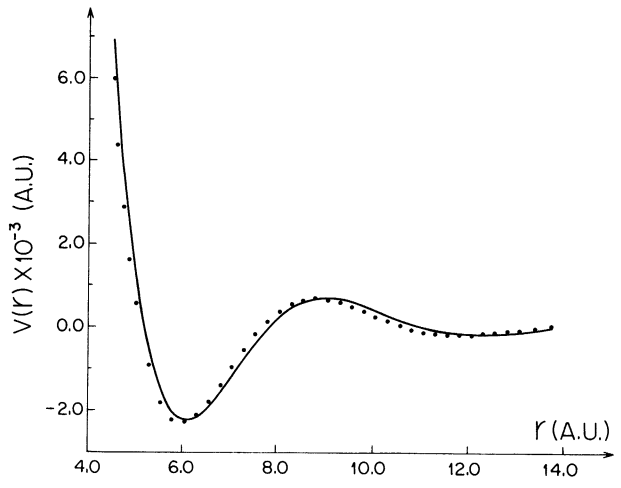

Fig. 3. — Calculated interionic potential for lithium. For a value of r_s corresponding to atmospheric pressure : —— ; for a value of r_s which is 4 % smaller than the corresponding value at atmospheric pressure : . . .

From the interionic potentials we calculated the phonon dispersion curves using the harmonic approximation for lithium and the self-consistent harmonic approximation for aluminium for every value of pressure. In figures 5 and 6 we show a comparison, for lithium and aluminium respectively, between experimental and calculated phonons at atmospheric pressure, and also the phonon dispersion curves for a value of r_s which is 4 % smaller than the corresponding value at atmospheric pressure. There is a good agreement between experimental and calculated phonons at atmospheric pressure. We could not find any phonon dispersion curves measurements for more values of pressure. We can see from figures 5 and 6 that the effect of pressure is to shift upwards the dispersion curves.

For lithium (for which the harmonic approximation is used) from the interionic potential, $V(r)$, we found k_1 and C_B by using equations (24) and (25). The elastic constants were found using equations (22) and (23). This was done for every value of pressure we considered, i.e. for every value of r_s we have considered.

For aluminium (for which the self-consistent harmonic approximation is used) we found the first guess of the set of force constants of the tensor force model using equations (23), (24) and (25). Then the convergence procedure was followed to obtain the force constants of the tensor force model self-consistently. This final set is used in equation (22) to calculate the elastic constants as functions of pressure.

Tables I and II show, for lithium and aluminium

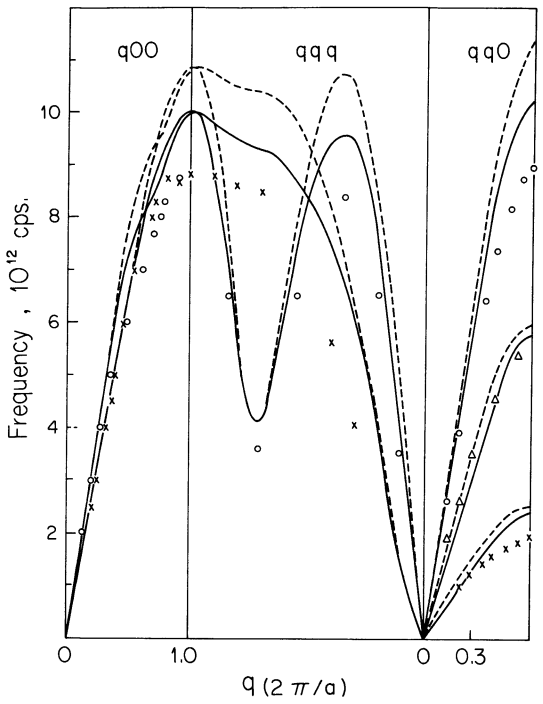

Fig. 5. — Phonon dispersion curves for lithium. Experimental results at atmospheric pressure [23] : ×, ○, △ ; calculated phonons at atmospheric pressure : —— ; calculated phonons for a value of r_s which is 4 % smaller than the corresponding value at atmospheric pressure : . . .

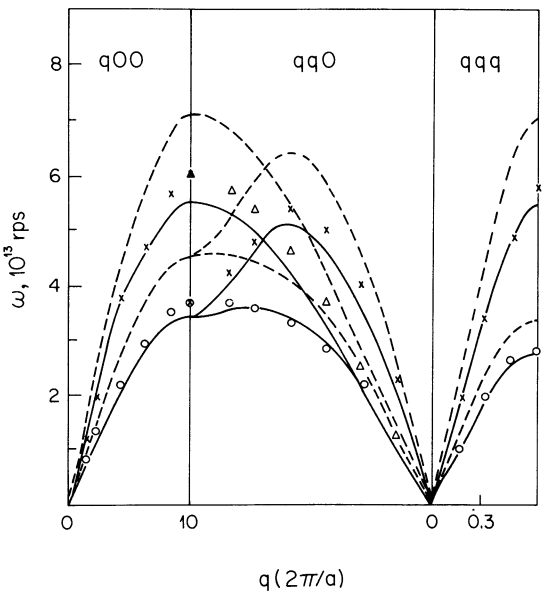

Fig. 6. — Phonon dispersion curves for aluminium. Experimental results at atmospheric pressure [24] : ×, ○, △ ; calculated phonons at atmospheric pressure : - - - ; calculated phonons for a value of r_s which is 4 % smaller than the corresponding value at atmospheric pressure : . . .

respectively, a comparison between experimental and calculated elastic constants at atmospheric pressure. There is a good agreement with experimental results. Notice that $C' = (C_{11} - C_{12})/2$ and $B = (C_{11} + 2\,C_{12})/3$.

There is another model which can be used with the method presented in this work and it is the spherical solid model, but in this model, the actual pseudopotential around the ion is mimicked by taking the spherical average of the host ion pseudopotential [9, 29]. This brings on additional complication to the problem, because if we want to know the spherical average of the host ion pseudopotential in our case,

Table I. — *Elastic constants for lithium at atmospheric pressure. We show the results of our calculation and the corresponding experimental values in* 10^{12} dynes/cm^2 ; *a) from reference* [25] ; *b) from reference* [26].

C_{11}	C_{11} exp	C_{12}	C_{12} exp	C_{44}	C_{44} exp	B	B exp	C'	C' exp
	0.1571[a]		0.1329[a]		0.116[a]		0.1410[a]		0.0121[a]
0.1459		0.1258		0.069		0.1325		0.01003	
	0.1471[a]		0.1245[a]		0.117[a]		0.11320[a]		0.0113[a]
			0.1102[b]		0.88[b]		0.117[b]		0.102[b]

Table II. — *Elastic constants for aluminium at atmospheric pressure. We show the results of our calculation and the corresponding experimental values* [27], *in* 10^{12} dynes/cm^2.

C_{11}	C_{11} exp	C_{12}	C_{12} exp	C_{44}	C_{44} exp	B	B exp	C'	C' exp
1.0890	1.143	0.46115	0.619	0.29463	0.316	0.67045	0.794	0.31394	0.262

we must know the solution to the problem, i.e. we must know the pseudopotential we are trying to find. In reference [9] the spherical average of the pseudopotential is calculated using an Ashcroft pseudopotential which is a phenomenological pseudopotential. This brings up another problem. With the inclusion of the phenomenological pseudopotential we cannot say that the pseudopotential found in reference [9] using the spherical solid model is from first principles. Additionally, the phonons generated from the model used in this work, at atmospheric pressure, are in much better agreement with experimental results than the phonons generated using the spherical solid model.

In tables III and IV we show the variation of the elastic constants with changes in volume. These volume changes are related to different values of applied pressure by interpolating the experimental results of reference [28]. We can see from these tables that the elastic constants, in general, increase when the pressure increases for both lithium and aluminium and, for the case of lithium, C' is not monotonically increasing with pressure. It seems to have a local maximum and a local minimum when the pressure is between 7.857 k atm and 12.73 k atm. This indicates that the difference between the shapes of C_{11} and C_{12} is not a simple function of pressure.

As a final comment, we have found that at atmospheric pressure, the elastic constants for aluminium and lithium, calculated from the first-principle, pressure-dependent, local pseudopotentials we are using in this work, are in good agreement with experimental results. This fact encouraged us to make a prediction of the pressure dependence of the elastic constants of these materials using the same pseudopotentials. The result of this prediction has the adequate physical behaviour. Unfortunately, we could not find experimental results for the range of values of pressure we have considered, so that this part of our calculation has still to be compared with experiment.

Table III. — *Pressure variation of the elastic constants of lithium. The correspondence between the volume variation and pressure was obtained by interpolating experimental results of reference* [28]. *The units of elastic constants are* 10^{12} dynes/cm^2.

P (10^4 atm)	$\Delta V/V$ %	C_{11}	C_{12}	C_{44}	B	C'
10^{-4}	0	0.14588	0.12583	0.06916	0.13251	0.01003
0.3650	− 3	0.15634	0.13437	0.07013	0.14169	0.01099
0.7857	− 6	0.16851	0.14565	0.07075	0.15327	0.01143
1.273	− 9	0.18052	0.15783	0.07100	0.16539	0.01135
1.818	− 12	0.19340	0.16748	0.07307	0.17612	0.01296
2.446	− 15	0.20546	0.17789	0.07451	0.18708	0.01379

Table IV. — *Pressure variation of the elastic constants of aluminium. The correspondence between the volume variation and pressure was obtained by interpolating experimental results of reference* [28]. *The units of elastic constants are* 10^{12} dynes/cm^2.

P (10^5 atm)	$\Delta V/V$ %	C_{11}	C_{12}	C_{44}	B	C'
10^{-5}	0	1.0890	0.46115	0.29463	0.67045	0.31394
0.2418	− 3	1.2113	0.51876	0.34647	0.74960	0.34627
0.6577	− 6	1.3470	0.58555	0.40301	0.83936	0.38071
1.024	− 9	1.4994	0.66164	0.46587	0.94090	0.41889
1.334	− 12	1.6632	0.72841	0.54096	1.0400	0.46740
1.609	− 15	1.8310	0.76148	0.63622	1.1180	0.53474

References

[1] VÁZQUEZ, G. J. and MAGAÑA, L. F., *J. Phys. France* **46** (1985) 2197.

[2] VÁZQUEZ, G. J. and MAGAÑA, L. F., *Rev. Mex. Fís.* **33** (1987) Feb., in press.

[3] HOHENBERG, H. and KOHN, W., *Phys. Rev.* **136** (1964) B 964.

[4] KOHN, W. and SHAM, L. J., *Phys. Rev. A* **140** (1965) 1133.

[5] MAGAÑA, L. F., *Phys. Lett. A* **80** (1980) 193.

[6] MAGAÑA, L. F., WHITMORE, M. D. and CARBOTTE, J. P., *Can. J. Phys.* **60** (1982) 424.

[7] MANNINEN, M., JENA, P., NIEMINEN, R. M., LEE, J. K., *Phys. Rev. B* **24** (1981) 7057.

[8] RASOLT, M. and TAYLOR, R., *Phys. Rev. B* **11** (1975) 2717.

[9] JENA, P., ESTERLING, D. M., MANNINEN, M., *J. Phys. F.* **14** (1984) 2017.

[10] BRYANT, G. W., MAHAN, G. D., *Phys. Rev. B* **17** (1978) 1744.

[11] ZAREMBA, E., ZOBIN, D., *Phys. Rev. Lett.* **44** (1980) 175.

[12] HARRISON, W. A., *Pseudopotentials in the theory of metals* (Benjamín, New York) 1966.

[13] GUNNARSON, O., LUNDQVIST, B. I., *Phys. Rev. B* **13** (1976) 4274.

[14] DUESBERY, M. S., TAYLOR, R., *Phys. Rev. B* **7** (1970) 2870.

[15] BORN, M., VON KARMAN, T., *Phys. Z.* **13** (1912) 297.

[16] BORN, M., VON KARMAN, T., *Phys. Z.* **14** (1913) 15.

[17] BOCCARA, N. and SARMA, G., *Physics* **1** (1965) 219.
[18] GILLIS, N. S., WERTHAMER, N. R., KOEHLER, T. R., *Phys. Rev.* **165** (1968) 951.
[19] COWLEY, E. R. and SHUKLA, R. C., *Phys. Rev. B* **4** (1974) 1261.
[20] TAOLE, S. H., GLUDE, H. R., TAYLOR, R., *Phys. Rev. B* **18** (1978) 2643.
[21] SQUIRES, G. L., *Ark. Fys.* **25** (1963) 21.
[22] SHUKLA, R. C., *J. Chem. Phys.* **45** (1966) 4178.
[23] SMITH, H. G., DOLLING, G., NIKLOW, R. M., VIJAYARAGHAVAN, P. R., WILKINSON, M. K., *Neutron Inelastic Scattering,* Vol. **1** (1968) p. 49.
[24] STEDMAN, R., NILSSON, G., *Phys. Rev.* **145** (1966) 492.
[25] SHIMADA, K., *Phys. Status Solidi* (b) **61** (1974) 325.
[26] JAIN, A. L., *Phys. Rev.* **123** (1961) 1234.
[27] KAMM, G. N., ALERS, G., *J. Appl. Phys.* **35** (1964) 327.
[28] BRIDGMAN, P. W., *Proc. Am. Acad. Arts. Sci.* **74** (1942) 425 ; **76** (1945) 1 ; **76** (1945) 9 ; **76** (1948) 71 ; **77** (1949) 189.
[29] ALMBLADH, C. O. and VON BARTH, V., *Phys. Rev. B* **13** (1976) 3307.